

# Chemical synthesis and characterization of maurocalcine, a scorpion toxin that activates $\text{Ca}^{2+}$ release channel/ryanodine receptors

Z. Fajloun<sup>a,\*</sup>, R. Kharrat<sup>b</sup>, L. Chen<sup>c</sup>, C. Lecomte<sup>a</sup>, E. Di Luccio<sup>a</sup>, D. Bichet<sup>d</sup>, M. El Ayeb<sup>b</sup>, H. Rochat<sup>a</sup>, P.D. Allen<sup>c</sup>, I.N. Pessah<sup>c</sup>, M. De Waard<sup>d</sup>, J.M. Sabatier<sup>a</sup>

<sup>a</sup>Laboratoire de Biochimie, CNRS UMR 6560, IFR Jean Roche, Faculté de Médecine Nord, Bd Pierre Dramard, 13916 Marseille Cedex 20, France

<sup>b</sup>Laboratoire des Venins et Toxines, Institut Pasteur de Tunis, P.O. Box 74, 1002 Belvédère, Tunis, Tunisia

<sup>c</sup>Department of Molecular Biosciences, School of Veterinary Medicine and Graduate Program in Neurosciences, One Shields Avenue, University of California, Davis, CA 95616, USA

<sup>d</sup>Laboratoire de Neurobiologie des Canaux Ioniques, INSERM U464, IFR Jean Roche, Faculté de Médecine Nord, Bd Pierre Dramard, 13916 Marseille Cedex 20, France

<sup>e</sup>Department of Anesthesia, Brigham and Women's Hospital, 75 Francis Street, Boston, MA 02115, USA

Received 3 January 2000; received in revised form 29 January 2000

Edited by Pierre Jolles

**Abstract** Maurocalcine is a novel toxin isolated from the venom of the chactid scorpion *Scorpio maurus palmatus*. It is a 33-mer basic peptide cross-linked by three disulfide bridges, which shares 82% sequence identity with imperatoxin A, a scorpion toxin from the venom of *Pandinus imperator*. Maurocalcine is peculiar in terms of structural properties since it does not possess any consensus motif reported so far in other scorpion toxins. Due to its low concentration in venom (0.5% of the proteins), maurocalcine was chemically synthesized by means of an optimized solid-phase method, and purified after folding/oxidation by using both C18 reversed-phase and ion exchange high-pressure liquid chromatographies. The synthetic product (sMCa) was characterized. The half-cystine pairing pattern of sMCa was identified by enzyme-based cleavage and Edman sequencing. The pairings were Cys3-Cys17, Cys10-Cys21, and Cys16-Cys32. In vivo, the sMCa was lethal to mice following intracerebroventricular inoculation ( $\text{LD}_{50}$ , 20  $\mu\text{g}/\text{mouse}$ ). In vitro, electrophysiological experiments based on recordings of single channels incorporated into planar lipid bilayers showed that sMCa potently and reversibly modifies channel gating behavior of the type 1 ryanodine receptor by inducing prominent subconductance behavior.

© 2000 Federation of European Biochemical Societies.

**Key words:** Maurocalcine; Scorpion toxin;  $\text{Ca}^{2+}$  release channel/ryanodine receptor; Synthetic peptide; Lipid bilayer

## 1. Introduction

Maurocalcine (MCa), a toxin from the venom of the Tunisian chactid scorpion *Scorpio maurus palmatus*, is a highly basic 33-mer peptide cross-linked by three disulfide bridges [1]. It shares about 82% sequence identity with imperatoxin A (IpTx A) [2,3], a scorpion toxin from the venom of *Pan-*

*dinus imperator*. MCa and IpTx A, although they are likely to adopt a grossly similar conformation, are peculiar in terms of their structural properties since they do not possess any consensus motif (which was reported to be shared by all scorpion toxins and insect defensins), and therefore are not thought to adopt the 'common'  $\alpha/\beta$  scaffold [4,5]. IpTx A was reported to activate  $\text{Ca}^{2+}$  release channel/ryanodine receptors of mammalian skeletal (RyR1) and cardiac muscles (RyR2) [6,7]. Together with inositol 1,4,5-triphosphate ( $\text{IP}_3$ ) receptors, RyR controls the intracellular  $\text{Ca}^{2+}$  permeability of various cell types, and is central in the process of excitation–contraction of muscle tissues [8]. Ligands such as toxins that specifically interact with RyR are molecular probes to investigate both the structure of the receptor and its role in excitation–contraction coupling. In the present work, we have chemically synthesized MCa by the Fmoc/*t*-butyl strategy [9], and carefully characterized the folded synthetic product sMCa for its physicochemical and electrophysiological properties. The disulfide bridge organization was formerly established by enzyme-based cleavage of sMCa followed by analyses of the proteolytic peptide fragments using mass spectrometry, amino acid content determination, and Edman sequencing techniques, as described [10,11]. sMCa was tested in vivo for lethal activity to [12], and by electrophysiology in vitro for its putative action on  $\text{Ca}^{2+}$  flux through RyR1 channels incorporated into planar bilayer lipid membranes. Our data demonstrate that sMCa is a new toxin active on RyR1 and that it binds onto a site different from that of ryanodine itself.

## 2. Materials and methods

### 2.1. Materials

*N*- $\alpha$ -Fmoc-L-amino acids, 4-hydroxymethylphenyloxy (HMP) resin, and reagents used for peptide synthesis were obtained from Perkin-Elmer. Solvents were analytical grade products from SDS. Enzymes (trypsin, and endoproteinase Asp-N) were obtained from Boehringer Mannheim.

### 2.2. Chemical synthesis of MCa and physicochemical characterization of the synthetic product, sMCa

The sMCa was obtained by the solid-phase method [9] using an automated peptide synthesizer (Model 433A, Applied Biosystems Inc.). Peptide chains were assembled stepwise on 0.25 mEq of HMP resin (1% cross-linked; 0.89 mEq of amino group/g) using 1 mmol of *N*- $\alpha$ -fluorenylmethyloxycarbonyl (Fmoc) amino acid derivatives. The side chain-protecting groups were: trityl for Cys and Asn; *tert*-butyl (for Ser, Thr, Glu, and Asp; pentamethylchroman for Arg, and *tert*-

\*Corresponding author. Fax: (33)-491 65 75 95.  
E-mail: fajloun.z@jean-roche.univ-mrs.fr

**Abbreviations:** HPLC, high-pressure liquid chromatography;  $\text{LD}_{50}$ , 50% lethal dose; MCa, maurocalcine, a scorpion toxin from the venom of *Scorpio maurus palmatus*; IpTx A, imperatoxin A, a scorpion toxin from the venom of *Pandinus imperator*; sMCa, synthetic maurocalcine; RyR1, type 1 ryanodine receptor; RyR2, type 2 ryanodine receptors; SR, sarcoplasmic reticulum; Tx2-9, a P-type  $\text{Ca}^{2+}$  channel blocker from the spider *P. nigriventer*

butyloxycarbonyl for Lys. *N*- $\alpha$ -Amino groups were deprotected by treatment with 18% and 20% (v/v) piperidine/*N*-methylpyrrolidone for 3 and 8 min, respectively. The Fmoc-amino acid derivatives were coupled (20 min) as their hydroxybenzotriazole active esters in *N*-methylpyrrolidone (four-fold excess). After peptide chain assembly, the peptide resin (about 1.8 g) was treated for 3 h at room temperature with a mixture of trifluoroacetic acid/H<sub>2</sub>O/thioanisole/ethanedithiol (88:5:5:2, v/v) in the presence of crystalline phenol (2.25 g). The peptide mixture was then filtered, and the filtrate was precipitated by adding cold *t*-butylmethyl ether. The crude peptide was pelleted by centrifugation (3000×*g*; 8 min) and the supernatant was discarded. The reduced peptide was then dissolved in 200 mM Tris–HCl buffer, pH 8.3, at a final concentration of 2.5 mM and stirred under air to allow oxidation/folding (72 h, room temperature). The target product, sMCA, was purified to homogeneity, first, by reversed-phase high-pressure liquid chromatography (HPLC) (Perkin-Elmer, C<sub>18</sub> Aquapore ODS 20  $\mu$ m, 250×10 mm) by means of a 60-min linear gradient of 0.08% (v/v) trifluoroacetic acid (TFA)/0–30% acetonitrile in 0.1% (v/v) TFA/H<sub>2</sub>O at a flow rate of 6 ml/min ( $\lambda$ =230 nm). A second step of purification of sMCA was achieved by ion exchange chromatography on a carboxymethyl cellulose matrix using 10 mM (buffer A) and 500 mM (buffer B) sodium phosphate buffers, pH 9 (60-min linear gradient from 0 to 60% buffer B at a flow rate of 1 ml/min). The homogeneity and identity of sMCA was assessed by: (i) analytical C<sub>18</sub> reversed-phase HPLC (Merck, C<sub>18</sub> Lichrospher 5  $\mu$ m, 4×200 mm) using a 60-min linear gradient of 0.08% (v/v) TFA/0–60% acetonitrile in 0.1% (v/v) TFA/H<sub>2</sub>O at a flow rate of 1 ml/min; (ii) amino acid analysis after acidolysis (6 N HCl/2% (w/v) phenol, 20 h, 118°C, N<sub>2</sub> atmosphere); and (iii) mass determination by matrix-assisted laser desorption ionization–time of flight mass spectrometry.

**2.3. Structural characterization of sMCA: assignment of half-cystine pairings by enzyme-based cleavage and Edman sequencing analysis**  
sMCA (600  $\mu$ g) was incubated either with trypsin or with endoprotease Asp-N at 10% (w/w) in 50 mM sodium phosphate, pH 7.4, for 20 h at 37°C. The peptide fragments were then purified by analytical reverse-phase HPLC (Merck, C<sub>18</sub> Lichrospher 5  $\mu$ m, 4×200 mm) with a 60-min linear gradient of 0.08% (v/v) TFA/0–60% acetonitrile in 0.1% (v/v) TFA/H<sub>2</sub>O at a flow rate of 1 ml/min ( $\lambda$ =230 nm), and freeze-dried prior to analysis. The peptide fragments were hydrolyzed by acidolysis (6 N HCl/phenol) and their amino acid content was analyzed (Beckman, System 6300 amino acid analyzer). The peptides were further characterized by mass spectrometry analysis (RP-DE Voyager, Perceptive Biosystems), and Edman sequencing using a gas-phase microsequencer (Applied Biosystems 470A). In standard HPLC conditions for analyzing phenylthiohydantoin (PTH) amino acid derivatives, diPTH-cystine elutes at a retention time of 9.8 min.

**2.4. Electrophysiological recordings**  
Cs<sup>+</sup> current through single RyR1 channels incorporated into planar lipid bilayers (BLM) was measured in an asymmetric CsCl (10:1 *cis*:*trans*) solution. The BLM was formed from a mixture of phosphatidylethanolamine and phosphatidylcholine (5:2, w/w) at 30–50 mg/ml in decane, across a 150–300  $\mu$ m aperture in a 1.0 ml polystyrene cup. Sarcoplasmic reticulum (SR) vesicles were added to the *cis* side of the chamber at a final concentration of 0.1–10  $\mu$ g/ml. The *cis* solution contained 500 mM CsCl, ~7  $\mu$ M CaCl<sub>2</sub>, 20 mM HEPES, pH 7.4, and the *trans* solution contained 50 mM CsCl, 7  $\mu$ M free Ca<sup>2+</sup>, 20 mM HEPES, pH 7.4. The monovalent cation Cs<sup>+</sup> was used as the perme-

ant ion instead of divalent cations (such as Ca<sup>2+</sup>) because of its better permeability through RyR1. After a single fusion event, sarcoplasmic reticulum (SR) vesicles in the *cis* chamber were quickly removed by perfusion with 9× volume of *cis* solution. Single-channel current was measured under voltage clamp using a Dagan 3900 amplifier (Dagan Instruments, Minneapolis, MN, USA). Holding potentials were with respect to the *trans* (ground) chamber, and positive current was defined as current flowing from *cis* to *trans*. Current signals were captured at 10 kHz and filtered at 1 kHz using a four-pole Bessel filter. Data were digitized with a Digidata 1200 interface (Axon Instruments, Burlingame, CA, USA) and stored on computer for subsequent analysis. Unless otherwise stated, test chemicals were sequentially added to the *cis* solution after an initial period of recording control channel behavior.

Single-channel activity was analyzed with pCLAMP 7.0 (Axon Instruments). Current levels were analyzed by mean variance analysis and peaks in the all-points amplitude histogram were fitted with Gaussian functions. The all-points amplitude histograms were constructed from selected segments of data 20–150 s in length to quantify the incidence of full and subconductance states.

### 3. Results

The amino acid sequence of MCA is shown in Fig. 1. MCA shares 82% sequence identity with IpTx A [3], 39% with agelenin [13] or Tx2-9 [14], and 27% with  $\omega$ -conotoxin MVIIC [15] (one scorpion toxin active on RyR1 and RyR2, two spider and one marine snail toxins that block presynaptic P-Q-type voltage-dependent Ca<sup>2+</sup> channels). It should be noted that the Cys residues are similarly arranged in all these peptides. Stepwise assembly of the peptide chains was achieved on 0.25 mmol HMP resin by means of optimized Fmoc/*t*-butyl chemistry [10,16]. The amount of target protected peptide linked to the resin was 0.20 mmol, which represents a yield of assembly of 80%. The profiles of elution by analytical C<sub>18</sub> reversed-phase HPLC of the crude reduced peptide after final acidolysis are shown in Fig. 2A. The crude peptide was folded/oxidized by 72 h exposure to air (oxygen as electron acceptor) (Fig. 2B), and purified to apparent homogeneity by preparative C<sub>18</sub> reversed-phase HPLC (Fig. 2C). As assessed by mass spectrometry, the purified fraction contained two peptides of experimental *M<sub>r</sub>* (*M*+*H*)<sup>+</sup> 3858.2 (sMCA; deduced *M<sub>r</sub>* (*M*+*H*)<sup>+</sup> 3858.5), and 3702.0 (sMCA missing an Arg residue; deduced *M<sub>r</sub>* (*M*+*H*)<sup>+</sup> 3702.3). Treatment of this fraction by ion exchange chromatography (Fig. 2D) resulted in the separation of the two components and final recovery of pure sMCA (Fig. 2E). As assessed by amino acid analysis, the net peptide content of dried sMCA was 75%. The final yield of sMCA synthesis (which combines peptide assembly, final acidolytic cleavage, folding/oxidation, two-step chromatographic purification) was about 2% (5  $\mu$ mol). Amino acid contents of sMCA (data not shown), as determined by amino

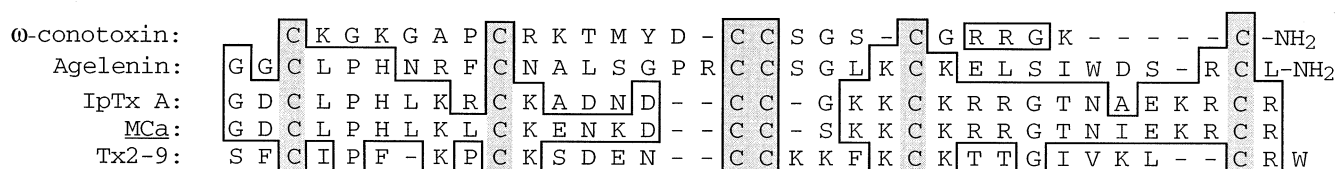


Fig. 1. Amino acid sequence (one-letter code) of MCA and comparison with other scorpion, spider, and marine snail toxin sequences. The amino acid sequences of  $\omega$ -conotoxin MVIIC from *Conus magus* marine snail [15], agelenin from *A. asperta* spider [13], IpTx A from *Pandinus imperator* scorpion [3], MCA (underlined) from *Scorpio maurus* palmatus scorpion [1], and Tx2-9 from *P. nigriventer* spider [14] were aligned using the Cys residues critical to the three-dimensional structures of the peptides. Gaps (-) were introduced in the amino acid sequences of these peptides to maximize homology. The positions of half-cystines are indicated in gray boxes. Amino acid sequence identities are enclosed in open boxes.

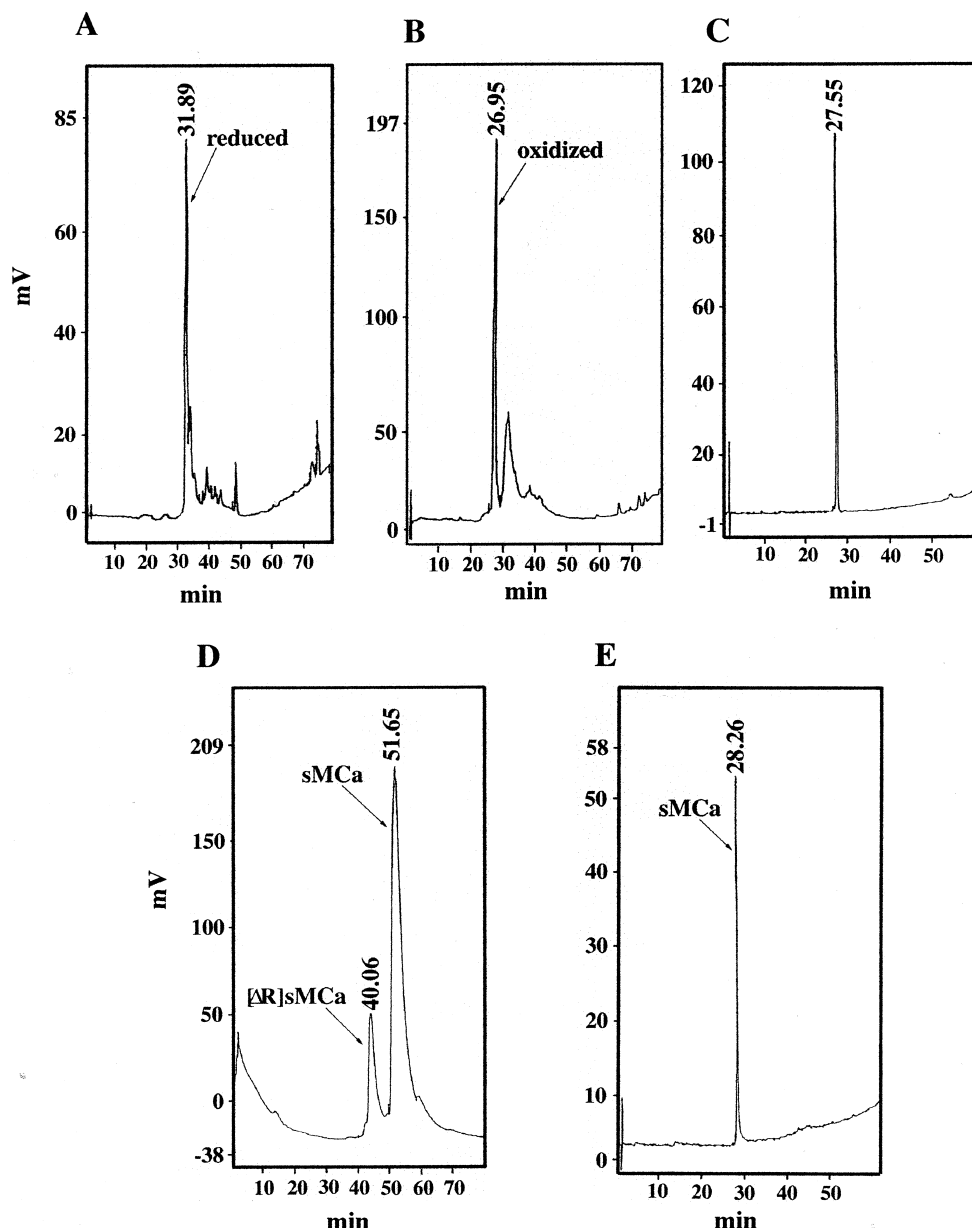


Fig. 2. Analytical  $C_{18}$  reversed-phase HPLC profiles of sMca at various stages of chemical synthesis and final purification of sMca. A: The crude reduced peptide after trifluoroacetic acid cleavage. B: The crude peptide after folding/oxidation. C: The peptide fraction –homogeneous but impure – collected after purification by  $C_{18}$  reversed-phase HPLC of the crude oxidized peptide. D: Cation exchange HPLC of the peptide fraction in C. As assessed by mass spectrometry analyses, the peaks at retention times of 44.06 min and 51.65 min correspond to sMca deleted of an Arg residue (by-product  $[\Delta R]sMca$ ) and sMca (target peptide), respectively. E: The purified sMca obtained after cation exchange HPLC of impure peptide fraction in C. For conditions, see Section 2.

acid analysis after acidolysis, and experimental  $M_r$  ( $M_r(M+H^+) = 3858.2$ ), were in agreement with the deduced values. To address half-cystine pairings, sMca was cleaved either with trypsin or with endoproteinase Asp-N, and the resulting proteolytic fragments were purified by HPLC, and characterized by means of amino acid analysis, mass spectrometry, and Edman sequencing techniques. The results of the individual enzyme treatments are summarized in Fig. 3. The half-cystine pairings were mapped as Cys3-Cys17, Cys10-Cys21, and Cys16-Cys32.

Next, we determined the physiological effect and molecular target of sMca. Intracerebroventricular injections of sMca produced lethal effects in mice. We found an  $LD_{50}$  value of

20  $\mu$ g per mouse, which is significantly less potent than scorpion toxins active on  $Na^+$  and  $K^+$  channels. This suggests that the potential molecular target was not a  $Na^+$  or a  $K^+$  channel. sMca had no significant sequence identity with any known scorpion toxin except IpTx A [3]. Since IpTx A targets RyR1 of skeletal muscle, we wanted to determine whether sMca was also active on this receptor. To test this hypothesis, we performed electrophysiological experiments on single RyR1 channels incorporated into planar lipid bilayers. The data illustrate that a nanomolar concentration of sMca applied on the *cis* side (cytoplasmic side) dramatically modified the channel gating behavior of RyR1 (Fig. 4, traces 1–8). No effect of the toxin was observed on the *trans* side (luminal

A

Enzyme	Retention time (min)	Proteolytic fragments	Half-cystine pairing determination
trypsin	18.9		Cys10 - Cys21
	19.8		
	20.5		
endoproteinase Asp-N	34.0		Cys3 - Cys17 Cys16 - Cys32

cleavage site

B

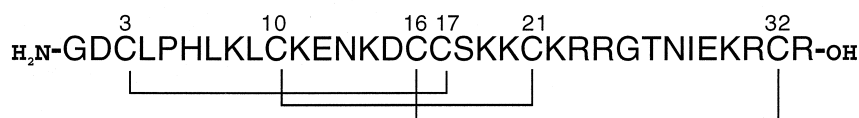


Fig. 3. Determination of the disulfide bridges of sMCA. A: Analysis of the peptide fragments obtained by proteolysis of sMCA using either trypsin or endoproteinase Asp-N. After enzyme-based cleavage, the peptide fragments were purified by analytical  $\text{C}_{18}$  reversed-phase HPLC and characterized by amino acid analysis, Edman sequencing and mass spectrometry. The peptide sequences deduced from these analyses are shown. Retention time in HPLC (left column) and established half-cystine pairings (right column) are indicated. B: Complete disulfide bridge pattern of sMCA as experimentally determined by enzyme-based cleavage. The positions of half-cystines (bold type) are indicated. The disulfide bridges are shown in lines.

side; data not shown) suggesting a cytoplasmic site of action of the toxin. Of the 12 channels tested, all exhibited similar responses to sMCA (5 nM to 1  $\mu\text{M}$ ) added to the *cis* chamber. The predominant action of sMCA was to rapidly induce long-lived subconductances, mainly having one-half the characteristic full conductance (traces 1–3). To a lesser extent, conductances approximating one-quarter the full conductance level were observed and were evident in the amplitude histograms. Four out of five channels modified by sMCA were shown to be subsequently modified by the alkaloid ryanodine (1  $\mu\text{M}$ ), confirming the identity of the channel as RyR1. Five out of six channels modified by sMCA were blocked by 10  $\mu\text{M}$  ruthenium red. With both sMCA and ryanodine present, RyR exhibited very stable and long-lived half- and quarter-subconductances approximating 50.5% and 29.3% of the characteristic control conductance level (trace 4). Once the channel was modified by sMCA and ryanodine, perfusion of the *cis* chamber only reversed the sMCA-induced quarter-states, whereas the ryanodine-mediated half-states persisted (trace 5), which indicates that ryanodine and sMCA are prob-

ably able to bind simultaneously and on separate sites onto the RyR1. Re-introduction of sMCA *cis* resulted in the rapid reappearance of the stable 51% and 29% conductance transitions (traces 6 and 7). Final addition of ruthenium red completely blocked the ryanodine/sMCA-modified channel (trace 8).

#### 4. Discussion

MCA is a 33-residue toxin isolated from the chactid scorpion *Scorpio maurus palmatus* [1]. It is present in minute amounts in a venom that is seldom collected, thereby precluding a functional analysis of its biological activity. Because natural MCA was not available in sufficient amounts to investigate its properties (structure and activity), we performed the chemical synthesis of this toxin by the solid-phase technique and fully characterized the synthetic compound.

Interestingly, MCA is peculiar in terms of structural properties since it does not possess any consensus motif reported so far in other scorpion toxins [4,5]. It does not fold according to

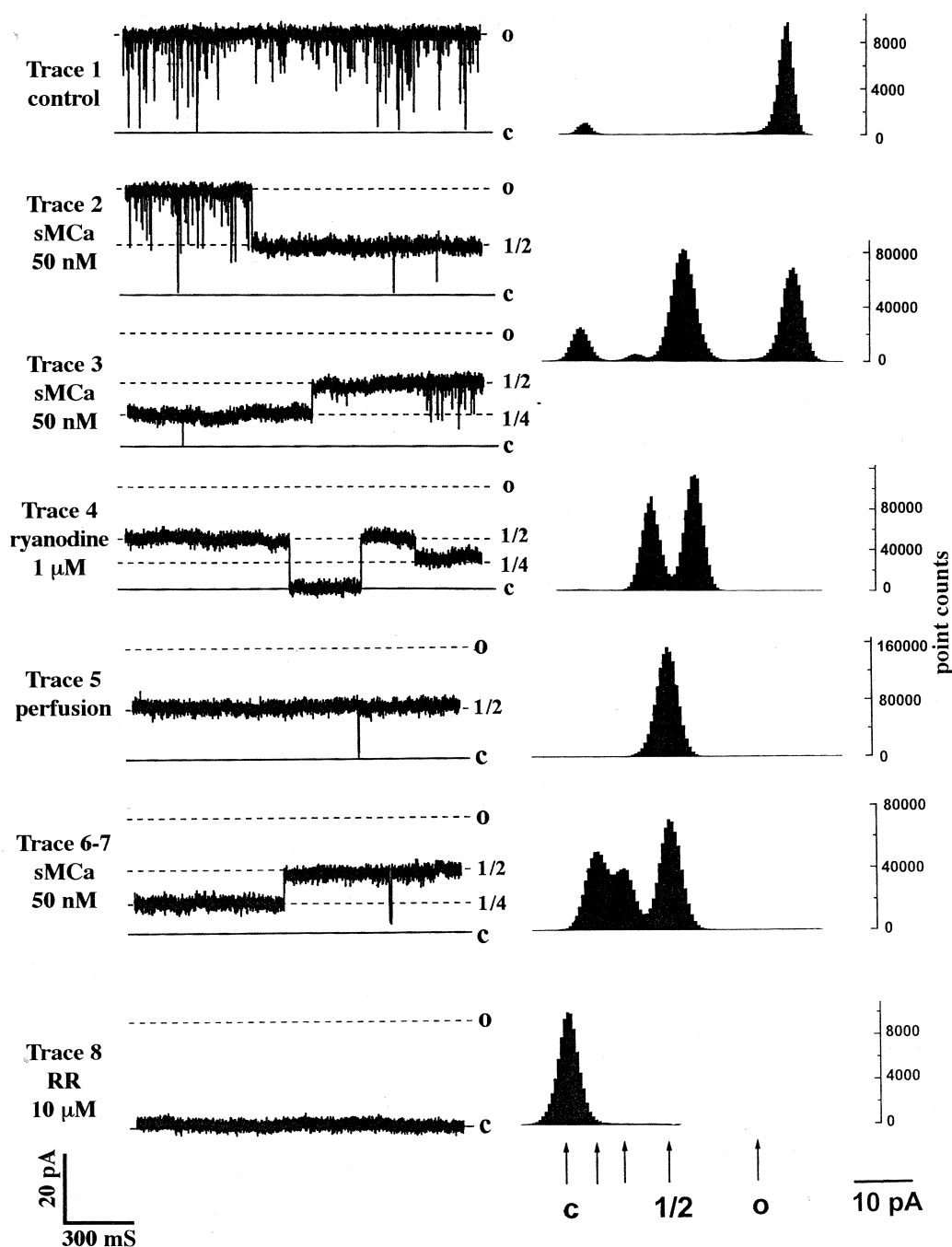


Fig. 4. Effects of sMCA on  $\text{Ca}^{2+}$  release channel/ryanodine receptors incorporated into planar lipid bilayers. sMCA stabilizes subconductance gating of RyR in a reversible manner. Single channel recording was performed in a 10:1 (*cis:trans*) CsCl solution at a holding potential of +30 mV. All traces are representative data traces from the same single channel. Trace 1: Control condition with 100  $\mu\text{M}$   $\text{Ca}^{2+}$  and 2 mM  $\text{ATPNa}_2$  *cis*. The full subconductance fluctuations predominated as indicated in the all-points amplitude histogram at the right. Traces 2 and 3: Addition of 50 nM sMCA (trace 2) induced long-lived subconductance gating behavior. The major subconductance induced by sMCA had an amplitude of 48% of that of full open amplitude. A subconductance having an amplitude approximately 29% of the full level was also evident in sMCA-modified channels (trace 3). Trace 4: Further addition of 1  $\mu\text{M}$  ryanodine to the sMCA-modified channel induced characteristic long half-conductance gating in addition to the smaller subconductance level (31.5%), indicating the coexistence of ryanodine and sMCA binding. Trace 5: Ryanodine and sMCA were removed from the *cis* chamber by perfusion with 9 $\times$  volume of drug-free solution (500 mM CsCl,  $\sim 7 \mu\text{M}$   $\text{Ca}^{2+}$ , 20 mM HEPES). After perfusion was complete, the channel exhibited only the half-conductance gating transitions as would be expected from irreversible modification by  $\mu\text{M}$  ryanodine. Traces 6 and 7: Subsequent re-introduction of 50 nM sMCA in the *cis* chamber induced the reappearance of smaller subconductance transitions with 19.7% and 29.9% of the full amplitude. Trace 8: Final addition of 10  $\mu\text{M}$  ruthenium red to the ryanodine/sMCA-modified channel completely eliminated gating activity.

the 'common'  $\alpha/\beta$  scaffold of toxins acting on either sodium, potassium and chloride channels [17,18]. In contrast, it was found that MCa folds according to the 'inhibitor cystine knot' motif which is also present in natural toxins acting on voltage-dependent  $\text{Ca}^{2+}$  channels such as spider and marine snail toxins (various  $\mu$ -agatoxins and  $\omega$ -conotoxins) [19,20]. The disulfide bridge pattern of sMCa was established by enzyme-based cleavage and analysis of the proteolytic peptide fragments thus obtained. The main difficulty in determining the half-cystine pairings of sMCa was the presence of a pair of contiguous half-cystines in positions 16 and 17, which did not permit cleavage between all the six half-cystines, and therefore prevented the use of the classical method of half-cystine pairing determination. Instead, the use of a new method [21] based on Edman sequencing has allowed formal identification of the three disulfide bridges. The disulfide bridges found in MCa linked half-cystines 3 and 17, 10 and 21 and 16 and 32. It should be noted that a similar disulfide bridge organization has been attributed to  $\omega$ -conotoxins active on voltage-dependent  $\text{Ca}^{2+}$  channels [22].

The structural homology of MCa with toxins from other animal species is further coupled with a similarity in functional activity since we found that the toxin acts on RyR1 isolated from skeletal muscle SR. It is striking that the apparent biological target of MCa is located intracellularly. However, it should be noted that this is not the first example of a scorpion toxin acting on RyR1. Scorpion toxin IpTx A is also a high-affinity activator of this channel type. This may not be so surprising since MCa shares 82% sequence identity with IpTx A. Also, it is likely that IpTx A folds according to a similar half-cystine pairing pattern as MCa although it has not been formally established in the case of this toxin. It is generally believed that these toxins are unable to cross the plasma membrane and that, therefore, the intracellular targets identified do not represent real targets but mimicking receptors. Notwithstanding, it should be emphasized that the extreme basicity of these toxins (e.g. MCa and IpTx A possess a net charge of +7 at physiological pH value) would make sMCa a good candidate to permeate the membrane [23]. It is also generally agreed that highly basic peptides translocate to the cytosol by locally disrupting the integrity of the lipid bilayer [24]. This membrane-crossing activity presumably results from an interaction of the positively charged moieties of basic residues with negatively charged polar heads of fatty acids of the plasma membrane.

Our data show that sMCa added to the cytoplasmic compartment (*cis* side of the skeletal RyR1) induces the appearance of subconductance states corresponding to about 51% and 29% of the typical full conductance seen with RyR1. A similar observation has been made for the action of IpTx A [25]. The data also suggest that the peptide is able to simultaneously bind to the RyR1 receptor together with ryanodine. This result was not surprising since it has been reported that IpTx A is capable of enhancing [ $^3\text{H}$ ]ryanodine binding [26]. Since sMCa induces the appearance of long-lived subconductance, in a similar though not identical manner as IpTx A, it is expected to induce net  $\text{Ca}^{2+}$  release from the SR. In this regard, sMCa differs from IpTx A in that it stabilizes multiple conductance states whereas the latter seems to favor only the 1/3 conductance state [25]. It has recently been noted that IpTx A shares structural homology with a segment of the II–III loop of the skeletal muscle dihydropyridine receptor

( $\alpha_{1S}$  subunit) that has been proposed to act as an activator of the RyR1. This homology concerns a cluster of basic amino acid residues (KKCKRR motif) at positions 19–24. Based on this observation, it was proposed that IpTx A is a peptide mimetic of the dihydropyridine receptor II–III loop, itself an endogenous effector structure that is crucial for excitation–contraction coupling. Remarkably, this basic motif was entirely conserved in MCa. The similarities in structure and function between IpTx A and MCa suggest that they may share the same binding site onto RyR1 and that this site could overlap a potential excitation–contraction signal transduction locus [26]. The binding site of IpTx A has been located to the cytoplasmic moiety of RyR1 between the clamp and handle domains [7], away from the transmembrane pore, supporting an allosteric mechanism of action of these toxins as opposed to the one involving direct positioning within the ion conducting channel. It is therefore expected that MCa will also be useful to study the molecular determinants of excitation–contraction coupling and the chain of conformational events leading to the opening of RyR1.

**Acknowledgements:** We wish to thank Dr. P. Mansuelle and S. Canarelli for running the protein sequencer and amino acid analyzer. We also thank Dr. H. Darbon for helpful discussion. Z. Fajloun is the recipient of a fellowship from the CNRS and the region Provence-Alpes-Côte d'Azur.

## References

- [1] Mosbah, A., Kharrat, R., Renisio, J.G., Blanc, E., Sabatier, J.M., El Ayeb, M. and Darbon, H. (1998) 6ème Rencontre en Toxinologie, Paris.
- [2] El Hayek, R., Lokuta, A.J., Arevalo, C. and Valdivia, H.H. (1995) *J. Biol. Chem.* 270, 28696–28704.
- [3] Zamudio, F.Z., Gurrola, G.B., Arevalo, C., Sreekumar, R., Walker, J.W., Valdivia, H.H. and Possani, L.D. (1997) *FEBS Lett.* 405, 385–389.
- [4] Bontems, F., Roumestand, C., Gilquin, B., Ménez, A. and Toma, F. (1991) *Science* 254, 1521–1523.
- [5] Bonmatin, J.M., Bonnat, J.L., Gallet, X., Vovelle, F., Ptak, M., Reichart, J.M., Hoffmann, J., Keppi, E., Legrain, M. and Achstetter, T. (1992) *J. Biomol. NMR* 2, 235–256.
- [6] Valdivia, H.H., Kirby, M.S., Lederer, W.J. and Coronado, R. (1992) *Proc. Natl. Acad. Sci. USA* 89, 12185–12189.
- [7] Samso, M., Trujillo, R., Gurrola, G.B., Valdivia, H.H. and Wengenkecht, T. (1999) *J. Cell Biol.* 146, 493–499.
- [8] Franzini-Armstrong, C. and Protasi, F. (1997) *Physiol. Rev.* 77, 699–729.
- [9] Merrifield, R.B. (1986) *Science* 232, 341–347.
- [10] Kharrat, R., Mabrouk, K., Crest, M., Darbon, H., Oughidini, R., Martin-Eauclaire, M.F., Jacquet, G., El Ayeb, M., Van Rietschoten, J., Rochat, H. and Sabatier, J.M. (1996) *Eur. J. Biochem.* 242, 491–498.
- [11] Sabatier, J.M., Lecomte, C., Mabrouk, K., Darbon, H., Oughidini, R., Canarelli, S., Rochat, H., Martin-Eauclaire, M.F. and Van Rietschoten, J. (1996) *Biochemistry* 35, 10641–10647.
- [12] Behrens, B. and Karber, C. (1935) *Arch. Exp. Pathol. Pharmacol.* 177, 379–388.
- [13] Hagiwara, K., Sakai, T., Miwa, A., Kawai, N. and Nakajima, T. (1990) *Biomed. Res.* 1, 181–186.
- [14] Cordeiro, M. do N., Diniz, C.R., Valentim, A. do C., Von Eickstedt, V.R., Gilroy, G. and Richardson, M. (1992) *FEBS Lett.* 310, 153–156.
- [15] Hillyard, D.R., Monje, V.R., Mintz, I.M., Bean, B.P., Nadasdi, L., Ramachandran, J., Miljanich, G., Azimi-Zoonooz, A., McIntosh, J.M. and Cruz, J.L. (1992) *Neuron* 9, 69–77.
- [16] Sabatier, J.M. (1999) in: *Handbook of Toxinology, Animal Toxins: Tools in Cell Biology* (Rochat, H. and Martin-Eauclaire M.F., Eds.), pp. 198–218, Birkhäuser Verlag, Basel.
- [17] Miller, C. (1995) *Neuron* 15, 5–10.

- [18] Darbon, H., Blanc, E. and Sabatier, J.M. (1999) in: Perspectives in Drug Discovery and Design: Animal Toxins and Potassium Channels (Darbon, H. and Sabatier, J.M., Eds.), Vols. 15/16, pp. 40–60, Kluwer/Escom, Dordrecht.
- [19] Narasimhan, L., Singh, J., Humblet, C., Guruprasad, K. and Blundell, T. (1994) *Nature Struct. Biol.* 1, 850–852.
- [20] Pallaghy, P.K., Nielsen, K.J., Craik, D.J. and Norton, R.S. (1994) *Protein Sci.* 3, 1833–1839.
- [21] Kharrat, R., Mansuelle, P., Sampieri, F., Crest, M., Oughidni, R., Van Rietschoten, J., Martin-Eauclaire, M.-F., Rochat, H. and El Ayebe, M. (1997) *FEBS Lett.* 406, 284–290.
- [22] Sevilla, P., Bruix, M., Santoro, J., Gago, F., Garcia, A.G. and Rico, M. (1993) *Biochem. Biophys. Res. Commun.* 192, 1238–1244.
- [23] Sabatier, J.M., Vives, E., Mabrouk, K., Benjouad, A., Rochat, H., Duval, A., Hue, B. and Barhaoui, E. (1991) *J. Virol.* 65, 961–967.
- [24] Mabrouk, K., Van Rietschoten, J., Vives, E., Darbon, H., Rochat, H. and Sabatier, J.M. (1991) *FEBS Lett.* 289, 13–17.
- [25] Trypathy, A., Resch, W., Xu, L., Valdivia, H.H. and Meissner, G. (1998) *J. Gen. Physiol.* 111, 679–690.
- [26] Gurrola, G.B., Arevalo, C., Sreekumar, R., Lokuta, A.J., Walker, J.W. and Valdivia, H.H. (1999) *J. Biol. Chem.* 274, 7879–7886.